



Low-Cost, Scalable Fabrication of All-Fabric Piezoresistive Sensors via Binder-Free, In-Situ Welding of Carbon Nanotubes on Bicomponent Nonwovens

Guangliang Tian¹ · Yihan Shi² · Jixia Deng¹ · Wenhua Yu¹ · Leihang Yang¹ · Yi Lu³ · Yi Zhao^{2,4} · Xiangyu Jin¹ · Qinfei Ke¹ · Chen Huang^{1,4} 

Received: 28 April 2023 / Accepted: 10 September 2023 / Published online: 3 November 2023
© Donghua University, Shanghai, China 2023

Abstract

Wearable piezoresistive sensors have shown enormous application prospects in flexible electronics and human–machine interfaces. However, current piezoresistive sensors suffer from common deficiencies including high fabrication cost, poor comfort and low attachment fastness of conductive substances on substrates, thereby impeding their large-scale production and practical use. Herein, a three-dimensional all-fabric piezoresistive sensor is reported based on coating multi-wall carbon nanotubes (MWCNTs) on bicomponent nonwovens composed of core-sheath fibers. The combination of core-sheath fibers with a heat-induced welding strategy greatly improves the adhesion fastness and stability of MWCNT network. The multi-layered all-fabric structure provides as-prepared sensors with high sensitivity ($9.43\% \text{ kPa}^{-1}$ in 0–10 kPa and $0.076\% \text{ kPa}^{-1}$ in 20–120 kPa), wide pressure-sensing range (0–120 kPa), fast response/relaxation time (100 and 60 ms), good reproducibility and air permeability. Application of the sensor is demonstrated through the detection of human activities (such as pulse, cough and joint movements) and the wireless monitoring of forefinger bending. Moreover, our sensor is fabricated out of cost-effective materials, using scalable approach without using glue or binders. The method established in this work may provide an efficient strategy for the design and production of high-performance all-fabric piezoresistive sensors.

Keywords Piezoresistive pressure sensors · Core-sheath fibers · All-fabric · Multi-wall carbon nanotubes · In-situ welding

Introduction

Wearable piezoresistive sensors have attracted immense research interests for their important application potential in flexible electronics [1, 2], speech recognition systems [3], healthcare monitoring [4, 5], human–machine interfaces [6] and intelligent robots [7]. Similar to mechanoreceptors of human skin, piezoresistive sensors featuring the excellent advantages of concise signal detection, high reliability, simple device configurations and low energy consumption are capable of sensing external mechanical stimuli through resistance or current change signals [8, 9]. Compared with metal foil gauges [10], conductive polymeric composites (CPCs) display greater potential in wearable piezoresistive sensors because of their light weight, good flexibility, and high sensitivity [11, 12]. A class of CPCs has been developed by blending conductive substances into an elastic polymer matrix [13–15]. As conductive substances are easily wrapped by insulative polymers, the proportion of conductive substances must be high enough to ensure the

✉ Yi Lu
luyi0718@126.com

✉ Qinfei Ke
kqf@dhu.edu.cn

✉ Chen Huang
hc@dhu.edu.cn

¹ State Key Laboratory for Modification of Chemical Fibers and Polymer Materials, College of Textiles, Donghua University, Shanghai 201620, China

² Shanghai Frontiers Science Center of Modern Textiles, Donghua University, Shanghai 201620, China

³ Department of Respiratory Medicine, Shanghai Jiao Tong University Affiliated Sixth People's Hospital, Shanghai 200233, China

⁴ Henan Key Laboratory of Medical and Protective Products, Henan Yadu Industry Co., Ltd., Xinxiang 453000, China

conductivity of CPCs, thus may inevitably affect the processing difficulty, cost, and flexibility of CPCs. The most commonly used strategy to resolve these problems is to uniformly coat flexible substrates with conductive substances, such as carbon nanotubes [16], graphene [17], MXene nanosheets [18], silver nanowires [19], poly(3,4-ethylenedioxythiophene):poly(styrenesulfonate) [20] and polyaniline [21].

To date, multifarious flexible substrates, including rubber films [22], sponges [23], papers [24], aerogels [25], leather-wear [26] and fabrics [27], have been employed for developing high-performance CPCs. Among them, fabric-based CPC (FCPC) is one of the most preferred candidates for wearable piezoresistive sensors, because of their exceptional flexibility, compressibility, breathability, and skin affinity [28–31]. The resistance change of FCPCs is mainly attributed to the microporous structure deformation of fabrics under external pressure. To satisfy the requirements for full-scale monitoring of both subtle physiological signals (e.g., pulse, breath and facial expression) and large activities (e.g., joint motions) from the human body, considerable efforts have been made to design FCPCs with outstanding compression resilience and large structural deformation [17, 20, 32]. This is because the large but stable architecture deformation of three-dimensional (3D) microporous FCPCs leads to a greater variation in conductive pathways, which is beneficial for increasing the sensitivity and sensing range of piezoresistive sensors [33].

Despite the encouraging advances of FCPCs, less attention has been paid to improving the adhesion fastness between conductive substances and fibers. Since conductive substances usually adhere to the fiber surface, the resultant sensor is vulnerable to the repeated exertion of wearing and washing in practical use. The subsequent loss of conductive substances causes an irreversible decrease in conductivity, thus impeding the long-term repeatability and service life of the sensor. While a trustworthy adhesion fastness of conductive coating on fabrics was reported in a few times [34–36], these reports required additional binders and/or a sophisticated fabrication approach, which hindered the broad applicability of resulting sensors. Moreover, most FCPC-based sensors contain polymeric films (such as polydimethylsiloxane (PDMS) and polylactic acid) [37, 38], but the airtight structure of these films may easily result in skin irritation and discomfort in daily usage. Therefore, it has been challenging to develop a binder-free, scalable technology for fabricating 3D all-fabric piezoresistive sensors with robust anchoring of conductive substances.

Herein, we demonstrate the facile fabrication of a 3D all-fabric piezoresistive sensor through dip-coating multi-wall carbon nanotubes (MWCNTs) on bicomponent spunbond nonwoven (NW) composed of core-sheath filaments with polypropylene (PP) as the core and polyethylene (PE) as the

sheath. The introduction of hydrophilic PP into PE component (fiber sheath) made the PE/PP spunbond NWs hydrophilic, which was conducive to the attachment of MWCNTs. An in-situ welding technology was adopted to enhance the attachment fastness between MWCNTs and PE/PP fibers. To construct large structural deformation that could increase the electric touchpoints and contact areas under pressure, multiple layers of 2D conductive NWs were laminated into 3D sensors. The relationship between the number of conductive fabric layers and the sensing performances of the sensor was systematically studied. The as-prepared sensor was proven effective in real-time detection of various types of human motions, such as pulse, breath, cough, muscle contraction and joint movement, and the detection was capable of being wireless.

Experimental Section

Materials

PE [melt index: 20 g/(10 min)] and PP [melt index: 35 g/(10 min)] polymer chips were provided by PetroChina, China. Hydrophilic PP (melt index: 25 g/(10 min)) polymer chips were purchased from Shanghai Huzheng Industrial, China. Commercial dispersants (XFZ20) were provided by Nanjing Xianfeng Nano Material Technology, China. MWCNTs (diameter = 10–20 nm, length < 30 μm) were obtained from Chengdu Organic Chemical, China.

Fabrication of PE/PP NW

PE and PP were melted and extruded by two screws to spinneret to form PE (sheath)/PP (core) melt fluid (the volume ratio of PE and PP was 50–50). A small proportion of hydrophilic PP (5 wt.%) was further blended with PE as the sheath component to change the wettability of PE/PP fibers. The temperature of both screws was 230 $^{\circ}\text{C}$, and the extrusion capacity of the metering pumps was 300 cc/min. High-speed cool air (speed = 20.1 m/s, temperature = 12 $^{\circ}\text{C}$) was used to quench and draw the melted polymer to form continuous PE/PP filaments with high strength. The filaments were further collected on a mesh apron (at a speed of 2 m/min) through negative pressure to obtain a fiber web. Finally, the formed fiber web was consolidated into NW (areal density = 36 g m^{-2}) through thermal bonding technology with a hot air temperature of 135 $^{\circ}\text{C}$.

Fabrication of MWCNT Dispersion

MWCNTs (0.2 g) were added into 100 mL of deionized water containing 0.08 g of XFZ20, followed by probe ultrasonication (Shanghai Bilang Instrument Manufacturing, China) for 2 h at a frequency of 20 kHz. The resultant

dispersion was gently centrifuged at a speed of 2000 r/min for 20 min to remove free MWCNTs.

Fabrication of NWs Coated with MWCNTs (MWCNT-NWs)

The as-prepared NW was immersed in the MWCNT dispersion for 10 min and dried in an air-circulating oven at 70 °C. The above coating procedure was repeated three times to acquire MWCNT-NWs with high conductivity. The MWCNT-NWs were then treated at different temperatures (120, 130 and 140 °C) in an air-circulating oven for 2.5 min. The resultant samples were labeled MWCNT-NW-120, MWCNT-NW-130 and MWCNT-NW-140.

Fabrication of Piezoresistive Sensors

The MWCNT-NWs were cut into squares with the dimensions of 1 cm × 1 cm × 0.08 cm (length × width × height). Five layers of MWCNT-NW-130 were stacked and then wrapped by a thin layer of spunbond NWs to construct a multi-layered piezoresistive sensor. To accurately detect the resistance signals of the sensor, two thin copper wires (diameter = 0.1 mm) were connected to its top and bottom layers by using conductive silver paste as the electrode. For comparison, 1-, 3- and 7-layered piezoresistive sensors were also fabricated.

Characterization

The surface and cross-sectional morphologies of the samples were observed by a SU8010 field-emission scanning electron microscope (FE-SEM, Hitachi, Japan). Raman spectra were obtained by an inViaReflex Raman system (Renishaw, UK) with 632 nm excitation in the range from 550 to 3200 cm^{-1} . The static water contact angle (WCA) was measured by an OCA15EC contact angle measuring system (Dataphysics, German), and air permeability was tested in an automatic permeability tester (Ningbo Textile Instrument, China). Thermal gravimetric analysis (TGA) was performed under a nitrogen atmosphere using a TGA 4000 thermogravimetric analyzer (PerkinElmer, USA) from 50 to 700 °C at a heating rate of 10 °C min^{-1} . The abrasion test was conducted by applying the Martindale measurement (Ningbo Textile Instrument, China) under a 200 g load for 600 cycles. The washing test was performed by stirring samples in deionized water for 30 h at a speed of 1000 r/min. The mechanical properties of the samples in cross-sectional direction (CD) and machine direction (MD) were characterized by a universal material tester (Shenzhen Suns Technology, China) according to the GB/T3923 strip method. Piezoresistive performances of sensors were measured by connecting the universal material

tester with a DAQ6510 data acquisition multimeter system (Keithley, USA). Current–voltage (I – V) curves were obtained by a Model 2450 source meter (Keithley, USA).

Sensitivity (S) of the sensor was calculated by Eq. (1):

$$S = \frac{|\Delta R/R_0|}{\Delta P} \quad (1)$$

where ΔP , ΔR and R_0 refer to the change in pressure, the relative change in resistance, and the initial resistance of the sensor without pressure, respectively. Depending on the change of resistance with pressure, sensitivity was categorized as S1 in the small pressure range (0–10 kPa) and S2 in the large pressure range (20–120 kPa), and was then fitted linearly to evaluate the sensing performances of the sensor. Additionally, to attain the response/relaxation time of the piezoresistive sensor, a compressing-holding-releasing cycle was performed, in which the holding time, loading pressure and loading/unloading speed were set as 3.1 s, 3 kPa and 100 mm/min, respectively.

Results and Discussion

Fabrication and Characterization of MWCNT-NWs

Figure 1a depicts the fabrication procedure for our multi-layered all-fabric piezoresistive sensors. The low melting temperature (T_m , ~ 130 °C) of PE enabled tight thermal bonding of neighboring fibers without applying any glue or binders. It also inspired us to realize the attachment fastness of MWCNTs on the surface of fibers facilitated by the PE sheath. To confirm our hypothesis, bicomponent NWs composed of core-sheath filaments with PP as the core and PE as the sheath were manufactured using industrialized spunbond technology. Owing to the hydrophobic nature of PE and PP, the as-prepared PE/PP NW displayed a high WCA of 136.8° (Fig. S1), which might block the penetration of MWCNT dispersion into the inter-fiber pores of NW. Hence, hydrophilic PP (5 wt.%) was introduced to change the wettability of PE/PP NW. It can be observed from Fig. 1b that fibers of the PE/PP NW presented a typical sheath-core cross-sectional structure. In thermal bonding, hot air (135 °C) passed through the fibrous web to partially melt the fiber sheath (PE) and bind adjacent fibers together, and the WCA of NW was 48.6° (Fig. 1c). In comparison with other modification technologies (chemical coating, plasma treatment, etc.) [39–41], the method of directly adding hydrophilic polymers in spinning process was particularly advantageous in durability. The resultant PE/PP NW became permanently hydrophilic, and its mechanical properties (Fig. 1d) were sufficient to meet the demands for wearable piezoresistive sensors.

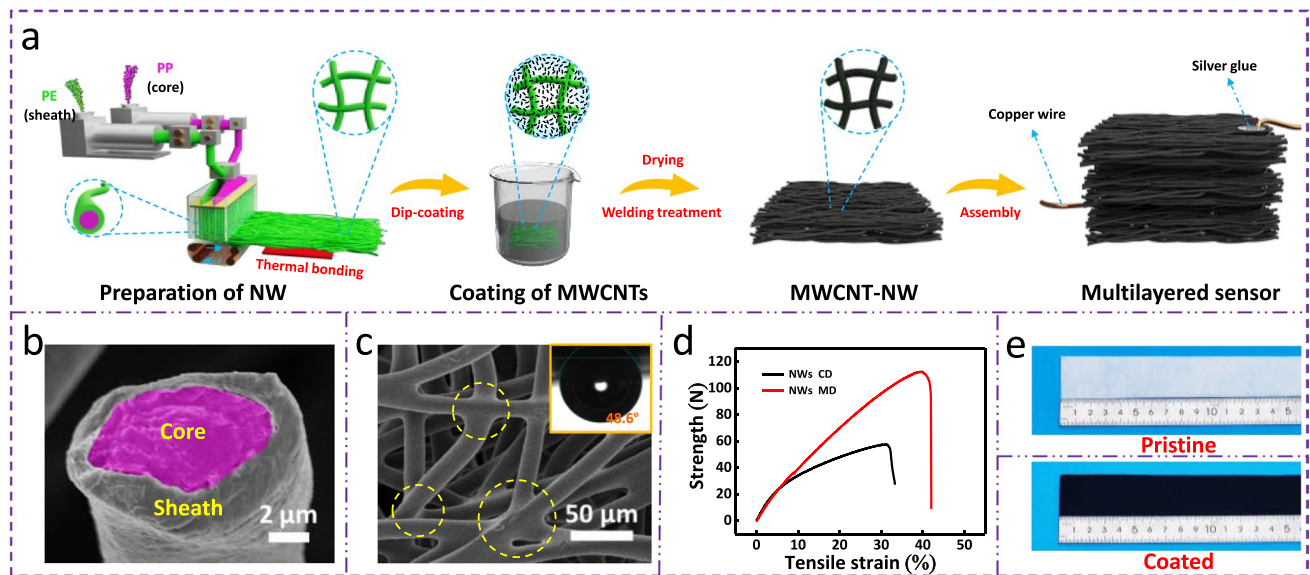


Fig. 1 **a** Schematic illustration for fabricating multi-layered all-fabric piezoresistive sensors. **b** FE-SEM image showing the sheath-core fiber structure. **c** FE-SEM image of NW. Inset is the WCA of NW.

The binding points of adjacent fibers are indicated by yellow circles. **d** Stress–strain curves of NW and **e** color of NWs before and after loading MWCNTs

The coating of MWCNTs was then triggered by repeatedly impregnating hydrophilic spunbond NWs in the MWCNT aqueous dispersion. After decorating with MWCNTs, the color of NWs changed from white to black, but the dimensions of NWs remained unchanged (Fig. 1e). For MWCNT-NWs, the interfacial connection between MWCNT network and PE/PP fibers mainly relied on van der Waals forces, and thus was vulnerable to repeated external forces such as wear and washing. This caused poor conductivity stability of MWCNT-NWs, which was usually associated with unfavorable durability of pressure sensors.

We developed an in-situ welding method to overcome this problem. According to the differential scanning calorimetry (DSC) endotherms of PE/PP spunbond NW (Fig. S2), we set the welding temperature at 120, 130, and 140 °C. Since the T_m of fiber core (PP) reached ~ 160 °C, the shape of the PE/PP fibers was well retained under these temperatures. When treated at 120 °C for 2.5 min, the MWCNT network could not be embedded into PE/PP fibers, and the surface morphology before and after treatment was highly comparable (Fig. 2a and b), suggesting that 120 °C was insufficient to embed MWCNTs into PE/PP fibers. When increasing the temperature to 130 °C, the MWCNT network was successfully welded into PE/PP fibers (Fig. 2c), which could be attributed to the low T_m of PE (~ 130 °C). The fiber sheath partially melted at this temperature, and a proportion of the MWCNTs on the fiber surface entered the fiber sheath due to the movement of the PE molecular chain. Therefore, the interfacial connections between MWCNTs and PE/PP fibers were greatly enhanced. When the temperature reached

140 °C, however, much of the PE was blended with the MWCNT network (Fig. 2d). Due to the insulative nature of PE, the connection of the MWCNT network was weakened, thus causing an increased volume resistance (Fig. 2e) that was not beneficial to the design of the piezoresistive sensors.

The influence of welding temperature on the attachment fastness between MWCNT network and PE/PP fibers was further examined by rubbing the MWCNT-NWs under a 200 g load and stirred washing of the MWCNT-NWs at 1000 r/min. Here, the relative resistance variation ($\Delta R/R_0$, where ΔR is the change in resistance under applied stimulation and R_0 is the initial resistance without stimulation) of MWCNT-NWs after repeated abrasion or washing was measured as a pivotal index to reflect the adhesion fastness of MWCNTs. After 600 rubbing cycles, the $\Delta R/R_0$ of MWCNT-NW-130 and MWCNT-NW-140 remained stable, but a clear increase in $\Delta R/R_0$ was found in MWCNT-NW-120, indicating a low adhesion fastness (Fig. 2f). The similar phenomenon was also found after continuous washing the sample for 30 h (Fig. 2g). These results proved that the heat-induced welding method was feasible and reliable for improving the adhesion fastness between MWCNTs and NWs. Due to the low volume resistance (4.53 k Ω) and high adhesion fastness, we selected 130 °C as the optimal welding temperature. The high adhesion fastness of MWCNTs at this temperature was further validated by the cross-sectional morphology of MWCNT-NW-130 (Fig. S3), in which distinct characteristic peaks of MWCNTs (1328, 1581, and 2644 cm^{-1}) were observed in Raman spectra (Fig. 2h).

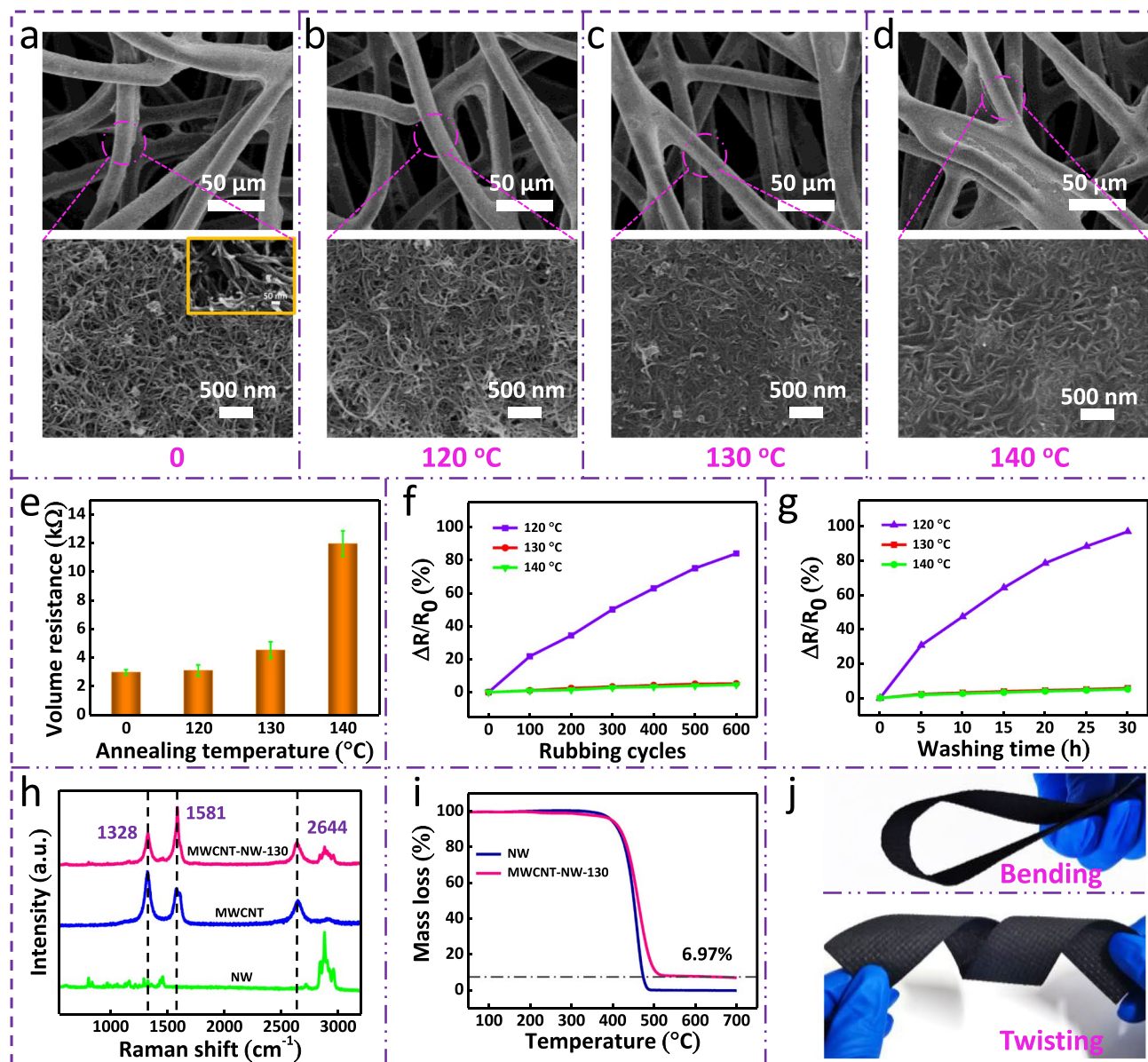


Fig. 2 **a** FE-SEM images of MWCNT-NWs without welding treatment. Inset is the FE-SEM image of MWCNTs. FE-SEM images of MWCNT-NWs treated with welding temperatures of **b** 120 °C, **c** 130 °C and **d** 140 °C for 2.5 min. **e** The relationship between welding temperature and volume resistance. $\Delta R/R_0$ changes of MWCNT-NWs

treated at different temperatures with **f** rubbing cycles and **g** washing time. **h** Raman spectra of pristine NW, MWCNT and MWCNT-NW-130. **i** TGA plots of pristine NW and MWCNT-NW-130. **j** Digital photographs displaying the flexibility of MWCNT-NW-130

TGA results in Fig. 2i suggested that the total proportion of MWCNTs on the PP/PE NW was 6.97%, which was much lower than those reported in previous methods [42, 43]. Considering the high price of MWCNTs (300 USD/kg), a low amount was used to reduce the cost. More importantly, the attachment of MWCNTs and subsequent welding treatment had no influence on the flexibility of MWCNT-NW-130 (Fig. 2j). To the best of our knowledge, this is the first time that heat-induced surface welding method was employed in PE/PP sheath-core fibers to enhance the adhesion fastness

of MWCNTs, as previous reports usually used single-component fibers as substrates, and therefore required additional binders that can reduce the initial flexibility and permeability of the fabric substrate [34, 44].

Assembly and Characterization of All-Fabric Piezoresistive Sensors

Because most fabrics are 2D (i.e., they are thin in the thickness direction) with limited structural deformation under

external pressure, the transformation of 2D fabrics into 3D fabrics with large but stable structural deformation is a significant step in designing fabric-based piezoresistive sensors. Toward this goal, up to seven layers of 2D MWCNT-NW-130 were stacked and assembled into 3D sensors with multi-layered architecture. The relationship between the number of MWCNT-NW-130 layers and the sensitivity of the sensor is illustrated in Fig. 3a. As the number of MWCNT-NW-130 layers increased from 1 to 7, the sensitivity of sensors in 0–10 kPa (small pressure range) and 20–120 kPa (large pressure range) increased. The sensitivity difference of sensors containing different layers of MWCNT-NW-130 could be attributed to the existence of inter-layer air gaps, which resulted in a relatively high resistance when no pressure was applied. Upon exposure to the applied pressure, these air gaps disappeared, leading to a rapid decrease in resistance. Consequently, when the number of layers increased from 1 to 7, the sensitivity of sensors in 0–10 kPa increased sharply. Air permeability of the sensors decreased

from 1382.12 to 465.57 mm/s with increasing MWCNT-NW-130 layers (Fig. 3b). To accurately detect both small and large motions from the human body, we selected a sensor with 5 layers of MWCNT-NW-130 for the following experiment. This sensor presented high sensitivity (9.43% and 0.076% kPa⁻¹ in 0–10 kPa and 20–120 kPa, respectively) and favorable air permeability (927.88 mm/s). The effects of immersion time were also studied, and the results indicated that both the volume resistance of MWCNT-NWs and the piezoresistive behavior of the sensor changed slightly when the immersion time exceeded 10 min (Fig. S4).

As we expected, the sensor was also capable of responding to dynamic pressure, and the corresponding variation in $\Delta R/R_0$ was highly repeatable under different applied pressures ranging from 0.25 to 80 kPa (Fig. 3c). It is worth noting that pressures smaller than 0.25 kPa might also be detected by our sensor, but the resolution limit of the dynamometer is 0.25 kPa. The response time of the sensor was ~100 ms under the pressure of 3 kPa, and the recovery

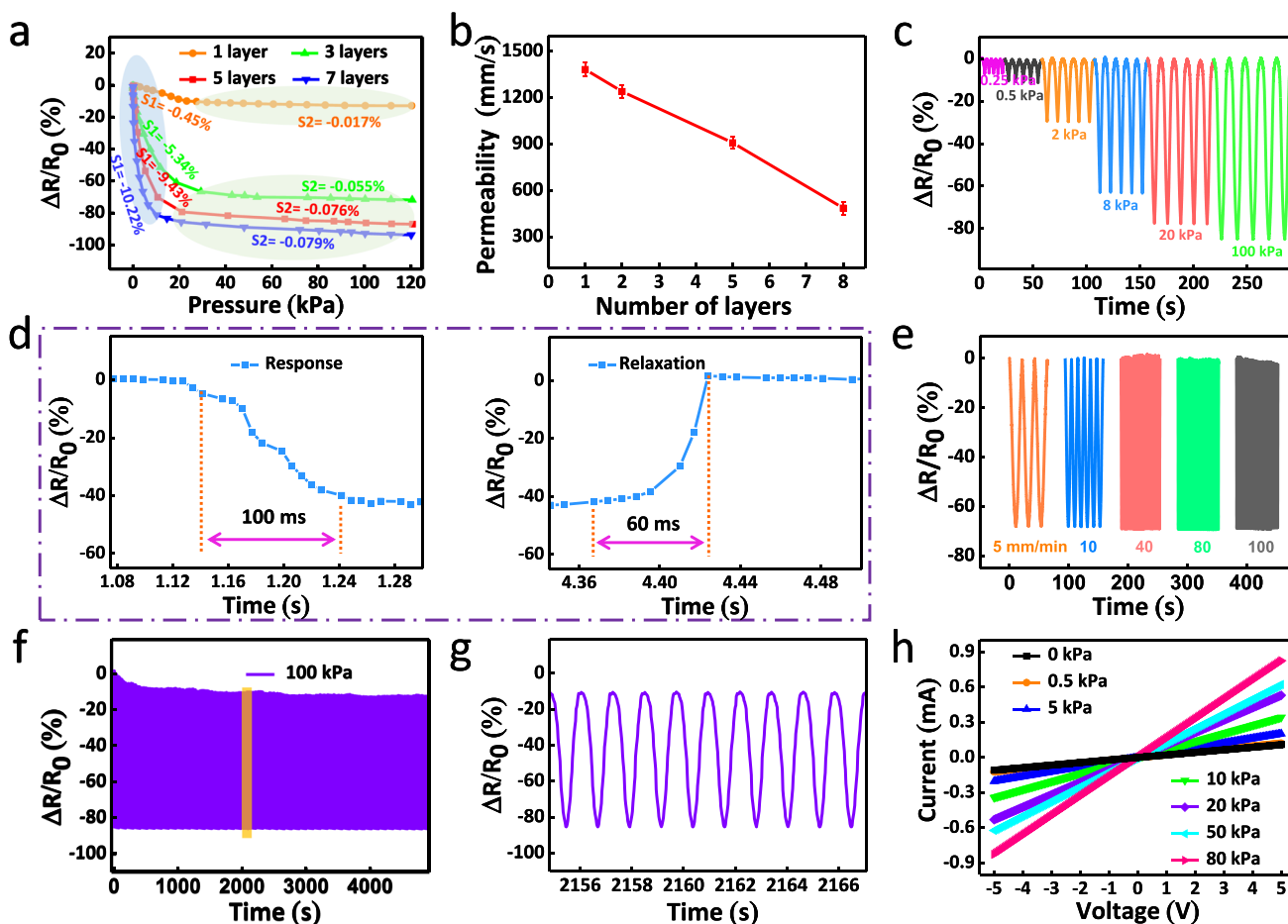


Fig. 3 a Resistance changes and b air permeability changes of sensors with different numbers of MWCNT-NW-130. c Resistance variation under various cyclic pressures. d Response time and relaxation time of the sensor. e Resistance response with a pressure of 10 kPa

at different frequencies. f Resistance response during 4000 repeated compression-release cycles with a pressure of 100 kPa, and g magnified waveforms drawn from f. h I–V characteristics of sensors at static pressure

time was ~ 60 ms (Fig. 3d). The $\Delta R/R_0$ change was stable when the rate of pressure loaded to the sensor increased from 5 to 100 mm/min (Fig. 3e). Repeated compression and release of 4000 cycles was further performed to evaluate the long-term durability of sensor. Figure 3f shows that a slight drop in $\Delta R/R_0$ was generated within the first 158 cycles, and the variation in $\Delta R/R_0$ became unapparent during the rest of the cycles (Fig. 3g). The initial drop in $\Delta R/R_0$ could be attributed to the small but permanent plastic deformation of the fiber-stacking structure under pressure, which was in accordance with the fabric-based piezoresistive sensors reported previously [33, 45]. The response capacity to static pressure was proven by I–V characteristics (Fig. 3h). The slopes of I–V curves increased linearly when increasing the static pressure (from 0.5 to 80 kPa), signifying the good “ohmic” behavior and the wide sensing range of our sensor.

Table 1 compares the basic performances (e.g., sensitivity, sensing range, response/relaxation time, reproducibility and air permeability) of our sensor with those of cutting-edge sensors [33, 46–54]. Deriving from the multi-layered all-fabric architecture and the high compressional resilience, our sensor exhibited exceptional overall performance. In particular, the large structural variation of the sensor enabled a high sensitivity, and a schematic illustration of the structural change under pressure is presented in Fig. 4a. With the exertion of a

small pressure, the decrease in the distance among MWCNT-NW-130 layers formed more electrical contact points among conductive fibers, resulting in a significant decrease in contact resistance and a high sensitivity in the range of 0–10 kPa. When the pressure ascended to a higher value, the MWCNT-NW-130 layers were all compressed, causing an increase in contact areas and a further decline in contact resistance. To more distinctly reflect the pressure-sensitive property, the sensor was coupled into a circuit composed of nine light-emitting diode bulbs and a power supply (3 V). The light intensity of bulbs became higher as the loaded weight increased from 20 to 200 g (Fig. 4b). Taken together, these results led us to conclude that the loose connections among the MWCNT-NW-130 layers of our multi-layered sensor were ideal for detecting the structural variation and the contact resistance change under pressure.

Real-Time Monitoring Human Motions Using All-Fabric Piezoresistive Sensors

We finally applied the sensors to different body parts to simultaneously detect both small and large human activities (Fig. 5a). The sensor attached to the volunteer’s wrist served as a monitor to capture the blood pulse signal of the radial artery, and a reproducible $\Delta R/R_0$ waveform with a

Table 1 A comparison of our sensor with previously reported pressure sensors

Pressure sensor	Materials	Sensitivity (kPa^{-1})	Sensing-range (kPa)	Stability (times)	Breathability (mm/s)
Ref 33	3D CNTs/NWs	0.057 0.00113	0–131.32	5000	553.85
Ref 46	Double-layered PDMS/CNTs	0.3 0.05	0–2	5000	airtight
Ref 47	3D polyurethane sponge coated with graphene and polyaniline	0.0021 0.0044 0.0109	0–25	10000	N/A
Ref 48	Electrospun carbon nanofiber films + PDMS films	0.96 0.12	0–2	3000	airtight
Ref 49	Multilayered graphene-paper + polyimide (PI) tape	0.172 0.001	0–20	300	airtight
Ref 50	Highly-oriented and free-standing CNTs sheets	0.0013 0.0004	0–40	6000	airtight
Ref 51	CNTs/PDMS sponge	0.033 0.008	0–150	200	N/A
Ref 52	Graphene/polyurethane sponge	0.26 0.03	0–10	1000	N/A
Ref 53	PEDOT:PSS/PI aerogels	0.021 0.054 0.019	0–17	200	N/A
Ref 54	PI nanofiber/MXene aerogel	0.14 0.002	0–85	1000	N/A
This work	Multilayered bicomponent NWs coated with CNTs	0.0943 0.00076	0–120	4000	927.88

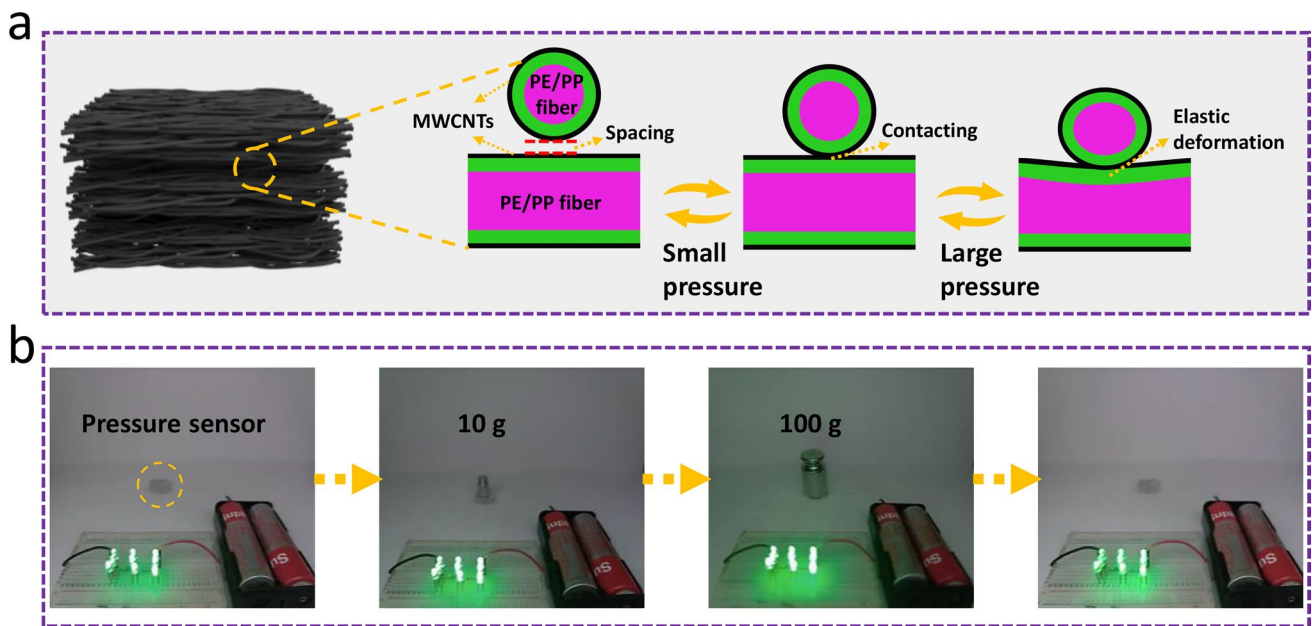


Fig. 4 **a** Schematic illustration showing the structural change of the sensor. **b** Resistance variation of the sensor under different loaded weights

periodicity of 84 times/min was acquired (Fig. 5b). The magnified wave of a single pulse displayed three typical characteristic peaks (Fig. 5c): the percussion wave (P), the tidal wave (T) and the diastolic wave (D). Based on the intensity of these peaks, the radial augmentation index (defined as T/P) could be calculated as an important reference for the evaluation of arterial stiffness and cardiovascular diseases. The radial augmentation index (0.76) was consistent with reference data for healthy men, suggesting the cardio-vascular fitness of the volunteer [48, 55]. The sensor-equipped mask detected a respiration rate of 19 times/min (Fig. 5d), while the sensor mounted on the throat successfully detected the muscle movements in cough (Fig. 5e). The sensor was also used to sense muscle contraction by making a fist. As exhibited in Fig. 5f, regular variation in $\Delta R/R_0$ could be acquired when the volunteer made a fist repeatedly, and the recorded waveforms were highly comparable. The high sensitivity and wide sensing range of our sensor further enabled the detection of knee joint movements. Bending speed of the knee joint was precisely reflected by different frequencies of $\Delta R/R_0$ (Fig. 5g). These findings supported the application potential of our sensor in noninvasive healthcare monitoring, wearable human–machine interfaces and physical training.

With the advent of the “Internet of Things” era, the transmission of signal waveforms to portable ports (e.g., mobile phones) has become increasingly important in applications such as medical wisdom [56]. Therefore, we connected the sensor with a microcontroller unit and a Bluetooth module for remote wireless monitoring (Fig. 5h). A smart glove loaded with our sensor was then developed to realize wireless

monitoring of finger bending. When bending a forefinger at a regular frequency, the real-time resistance variation successfully emerged on the screen of a mobile phone (Fig. 5i and movie S1). The resistance variation during the whole bending process was regular, steady and highly distinguishable (Fig. 5j).

Pressure sensors should be manufactured by using cost-effective materials and scalable fabrication techniques. The PP/PE NW substrates in our sensor have been extensively used in medical supplies (such as masks and surgical gowns) at a cost of 0.1 USD/m². Although the prices of MWCNTs are high (300 USD/kg), their proportion was only 6.97% of the total mass of our sensors. In addition, the fabrication approaches in this work, including spunbond, solution coating and welding treatment have all been industrialized, without involving sophisticated facilities or time-consuming procedures. Therefore, the overall cost of our sensor (1 cm²) was only ~0.02 USD, which is readily affordable in most applications.

Conclusions

In summary, we report the low-cost and scalable fabrication of a 3D all-fabric piezoresistive sensor based on PP/PE bicomponent nonwoven and MWCNTs. The combination of core-sheath fibers and a binder-free, in-situ welding strategy greatly enhanced the adhesion fastness of the MWCNT network. The multi-layered fabric architecture provided the sensor with high sensitivity, wide pressure-sensing range, fast response/relaxation, excellent long-term durability and

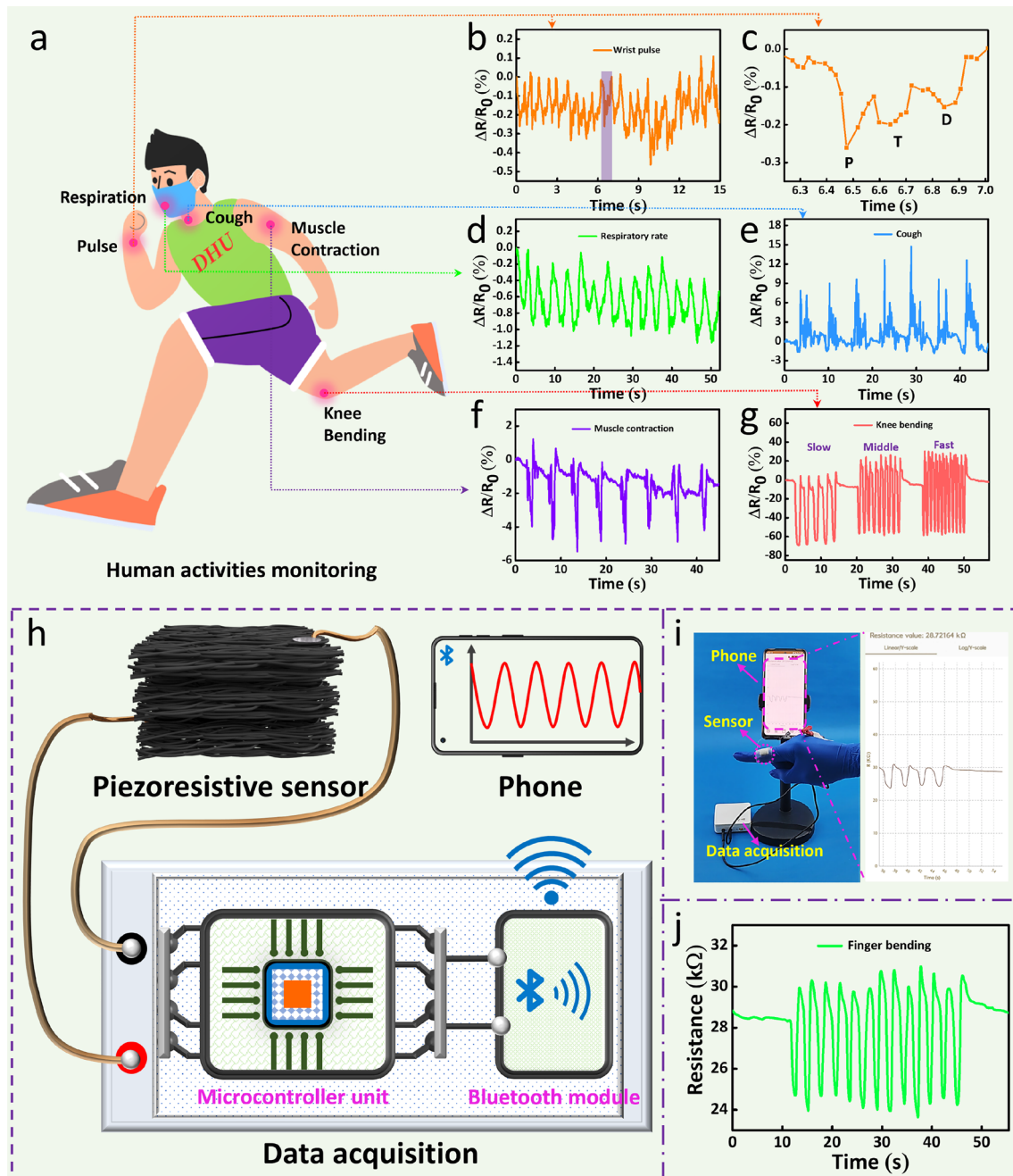


Fig. 5 **a** Diagram showing motion detection from human body parts. **b** Captured $\Delta R/R_0$ signals of wrist pulse and **c** enlarged waveform from one pulse signal. Regular $\Delta R/R_0$ signals resulting from **d** respiration and **e** cough. Reproducible $\Delta R/R_0$ signals of **f** muscle contraction and **g** knee bending. **h** Diagram demonstrating the concept of remote wireless monitoring using the sensor. **i** Digital photograph

showing both detection of forefinger bending and wireless transmission of resistance signals. Magnified photograph is the corresponding real-time resistance variation signals transmitted wirelessly to a mobile phone. **j** Recorded resistance variation during the whole process of forefinger bending

good air permeability, and thus the sensor could be applied for real-time detection of various human activities. Remote wireless monitoring of forefinger bending was also achieved. We propose that the facile, versatile, low-cost and scalable approach developed in this work may ultimately lead to the

manufacture and application of commercialized fabric-based pressure sensors.

Supplementary Information The online version contains supplementary material available at <https://doi.org/10.1007/s42765-023-00331-2>.

Acknowledgements Financial supports from the National Natural Science Foundation of China (Grant No. 32271378), Henan Key Laboratory of Medical and Protective Products (No. YDFH-2022-KF-02), and the Fundamental Research Funds for the Central Universities and Graduate Student Innovation Fund of Donghua University (CUSF-DH-D-2020019) are acknowledged.

Data availability The data that support the findings of this study are available from the corresponding author upon reasonable request.

Declarations

Conflict of Interest The authors declare that they have no known competing financial interests or personal relationships that could have appeared to influence the work reported in this paper.

References

- Tang XY, Yang WD, Yin SR, Tai GJ, Su M, Yang J, Shi HF, Wei DP, Yang J. Controllable graphene wrinkle for a high-performance flexible pressure sensor. *ACS Appl Mater Interfaces*. **2021**;13:20448.
- Wang N, Yang X, Zhan XX. Ultrarobust subzero healable materials enabled by polyphenol nano-assemblies. *Nat Commun*. **2023**;14:814.
- Lee S, Kim J, Yun I, Bae G, Kim D, Park S, Yi IL-M, Moon W, Chung Y, Cho K. An ultrathin conformable vibration-responsive electronic skin for quantitative vocal recognition. *Nat Commun*. **2019**;10:2468.
- Luo Y, Miao YP, Wang HM, Dong K, Hou L, Xu YY, Chen WC, Zhang Y, Zhang YY, Fan W. Laser-induced Janus graphene/poly(p-phenylene benzobisoxazole) fabrics with intrinsic flame retardancy as flexible sensors and breathable electrodes for fire-fighting field. *Nano Res*. **2023**;16:760.
- Wang Y, Shu R, Zhang XX. Strong, supertough and self-healing biomimetic layered nanocomposites enabled by reversible interfacial polymer chain sliding. *Angew Chem Int Ed*. **2023**;62:e202303446.
- Lu DX, Liao SQ, Chu Y, Cai YB, Wei QF, Chen KL, Wang QQ. Highly durable and fast response fabric strain sensor for movement monitoring under extreme conditions. *Adv Fiber Mater*. **2023**;5:223.
- Feng B, Zou GS, Wang WG, Dong MG, Xiao Y, Ren H, Zhao XL, Zhao GL, Wu AP, Zhu HW, Liu L. A programmable, gradient-composition strategy producing synergistic and ultrahigh sensitivity amplification for flexible pressure sensing. *Nano Energy*. **2020**;74: 104847.
- He YX, Wu DY, Zhou MY, Zheng YJ, Wang TF, Lu C, Zhang L, Liu H, Liu CT. Wearable strain sensors based on a porous polydimethylsiloxane hybrid with carbon nanotubes and graphene. *ACS Appl Mater Interfaces*. **2021**;13:15572.
- Xu DW, Ouyang ZF, Dong YJ, Yu HY, Zheng S, Li SH, Tam KC. Robust, breathable and flexible smart textiles as multifunctional sensor and heater for personal health management. *Adv Fiber Mater*. **2023**;5:282.
- Han ST, Peng HY, Sun QJ, Venkatesh SS, Chung KS, Lau SC, Zhou Y, Roy VAL. An overview of the development of flexible sensors. *Adv Mater*. **2017**;29:1700375.
- Wang L, Huang XW, Wang D, Zhang WM, Gao SJ, Luo JC, Guo Z, Xue HG, Gao JF. Lotus leaf inspired superhydrophobic rubber composites for temperature stable piezoresistive sensors with ultrahigh compressibility and linear working range. *Chem Eng J*. **2021**;405: 127025.
- Wang L, Wang D, Wu ZF, Luo JC, Huang XW, Gao Q, Lai XJ, Tang LC, Xue HG, Gao JF. Self-derived superhydrophobic and multifunctional polymer sponge composite with excellent joule heating and photothermal performance for strain/pressure sensors. *ACS Appl Mater Interfaces*. **2020**;12:13316.
- Zhou HW, Wang ZW, Zhao WF, Tong XM, Jin XL, Zhang XC, Yu Y, Liu HB, Ma YC, Li SS, Chen WX. Robust and sensitive pressure/strain sensors from solution processable composite hydrogels enhanced by hollow-structured conducting polymers. *Chem Eng J*. **2021**;403: 126307.
- Jung S, Kim JH, Kim J, Choi S, Lee J, Park I, Hyeon T, Kim DH. Reverse-micelle-induced porous pressure-sensitive rubber for wearable human-machine interfaces. *Adv Mater*. **2014**;26:4825.
- Ma C, Wang M, Wang K, Uzabakirih PC, Chen X, Zhao G. Ultrasensitive, highly selective, integrated multidimensional sensor based on a rigid-flexible synergistic stretchable substrate. *Adv Fiber Mater*. **2023**. <https://doi.org/10.1007/s42765-023-00274-8>.
- Du DH, Tang ZH, Ouyang JY. Highly washable e-textile prepared by ultrasonic nanosoldering of carbon nanotubes onto polymer fibers. *J Mater Chem C*. **2018**;6:883.
- Lu YJ, Tian MW, Sun XT, Pan N, Chen FX, Zhu SF, Zhang XS, Chen SJ. Highly sensitive wearable 3D piezoresistive pressure sensors based on graphene coated isotropic non-woven substrate. *Compos Part A: Appl S*. **2019**;117:202.
- Fu XY, Li JZ, Li DD, Zhao LJ, Yuan ZY, Shulga V, Han W, Wang LL. MXene/ZIF-67/PAN nanofiber film for ultra-sensitive pressure sensors. *ACS Appl Mater Interfaces*. **2022**;14:12367.
- Peng SH, Wu SY, Yu YY, Xia BJ, Lovell NH, Wang CH. Multimodal capacitive and piezoresistive sensor for simultaneous measurement of multiple forces. *ACS Appl Mater Interfaces*. **2020**;12:22179.
- Li MF, Chen JX, Zhong WB, Luo MY, Wang W, Qing X, Lu Y, Liu QZ, Liu K, Wang YD, Wang D. Large-area, wearable, self-powered pressure-temperature sensor based on 3D thermoelectric spacer fabric. *ACS Sens*. **2020**;5:2545.
- Yang T, Deng WL, Chu X, Wang X, Hu YT, Fan X, Song J, Gao YY, Zhang BB, Tian G, Xiong D, Zhong S, Tang LH, Hu YH, Yang WQ. Hierarchically microstructure-bioinspired flexible piezoresistive bioelectronics. *ACS Nano*. **2021**;15:11555.
- Cheng YF, Ma YN, Li LY, Zhu M, Yue Y, Liu WJ, Wang LF, Jia SF, Li C, Qi TY, Wang JB, Gao YH. Bioinspired microspines for a high-performance spray $Ti_3C_2T_x$ MXene-based piezoresistive sensor. *ACS Nano*. **2020**;14:2145.
- Zhang H, Liu NS, Shi YL, Liu WJ, Yue Y, Wang SL, Ma YN, Wen L, Li LY, Long F, Zou ZG, Gao YH. Piezoresistive sensor with high elasticity based on 3D hybrid network of Sponge@CNTs@Ag NPs. *ACS Appl Mater Interfaces*. **2016**;8:22374.
- Guo Y, Zhong MJ, Fang ZW, Wan PB, Yu GH. A Wearable transient pressure sensor made with MXene nanosheets for sensitive broad-range human-machine interfacing. *Nano Lett*. **2019**;19:1143.
- Wang SJ, Meng WY, Lv HF, Wang ZX, Pu JW. Thermal insulating, light-weight and conductive cellulose/aramid nanofibers composite aerogel for pressure sensing. *Carbohydr Polym*. **2021**;270: 118414.
- Zou BH, Chen YY, Liu YH, Xie RJ, Du QJ, Zhang T, Shen Y, Zheng B, Li S, Wu JS, Zhang WN, Huang W, Huang X, Huo FW. Repurposed leather with sensing capabilities for multifunctional electronic skin. *Adv Sci*. **2019**;6:1801283.
- Li SM, Wu GZ, Hu YJ, Fang MQ, He LX, He Y, Xiao XL. Preparation of pressure distribution monitoring socks and related sensing properties. *Fangzhi Xuebao/J Text Res*. **2019**;40:138.
- Ma JJ, Zhang N, Cheng Y, Kou XR, Niu YW, Jin XY, Ke QF, Zhao Y. Green fabrication of multifunctional three-dimensional

- superabsorbent nonwovens with thermo-bonding fibers. *Adv Fiber Mater.* **2022**;4:293.
29. Fan W, Zhang C, Liu Y, Wang SJ, Dong K, Li Y, Wu F, Liang JH, Wang CL, Zhang YY. An ultra-thin piezoelectric nanogenerator with breathable, superhydrophobic, and antibacterial properties for human motion monitoring. *Nano Res.* **2023**. <https://doi.org/10.1007/s12274-023-5413-8>.
 30. Tian MW, Li ZQ, Lu YJ, Zhu SF, Zhang XS, Qu LJ. Recent progress of textile-based flexible mechanical sensors. *Fangzhi Xuebao/J Text Res.* **2018**;39:170.
 31. Shi YH, Tian GL, Ni RY, Zhang L, Hu WF, Zhao Y. Facile and green lyocell/feather nonwovens with in-situ growth of ZIF-8 as adsorbent for physicochemical CO₂ capture. *Sep Purif Technol.* **2023**;322: 124356.
 32. Zhang L, Li HQ, Lai XJ, Gao TY, Yang J, Zeng XR. Thiolated graphene@polyester fabric-based multilayer piezoresistive pressure sensors for detecting human motion. *ACS Appl Mater Interfaces.* **2018**;10:41784.
 33. Tian GL, Zhan L, Deng JX, Liu HG, Li J, Ma JJ, Jin XY, Ke QF, Huang C. Coating of multi-wall carbon nanotubes (MWCNTs) on three-dimensional, bicomponent nonwovens as wearable and high-performance piezoresistive sensors. *Chem Eng J.* **2021**;425: 130682.
 34. Yang LY, Ma J, Zhong WB, Liu QZ, Li MF, Wang W, Wu Y, Wang YD, Liu X, Wang D. Highly accurate fabric piezoresistive sensor with anti-interference from both high humidity and sweat based on hydrophobic non-fluoride titanium dioxide nanoparticles. *J Mater Chem C.* **2021**;9:5217.
 35. Ma C, Yuan Q, Du HS, Ma MG, Si CL, Wan PB. Multiresponsive MXene (Ti₃C₂T_x)-decorated textiles for wearable thermal management and human motion monitoring. *ACS Appl Mater Interfaces.* **2020**;12:34226.
 36. Cao XY, Zhang J, Chen SW, Varley RJ, Pan K. 1D/2D nanomaterials synergistic, compressible, and response rapidly 3D graphene aerogel for piezoresistive sensor. *Adv Funct Mater.* **2020**;30:2003618.
 37. Liu MM, Pu X, Jiang CY, Liu T, Huang X, Chen LB, Du CH, Sun JM, Hu WG, Wang ZL. Large-area all-textile pressure sensors for monitoring human motion and physiological signals. *Adv Mater.* **2017**;29:1703700.
 38. Zheng YJ, Yin R, Zhao Y, Liu H, Zhang DB, Shi XZ, Zhang B, Liu CT, Shen CY. Conductive MXene/cotton fabric based pressure sensor with both high sensitivity and wide sensing range for human motion detection and E-skin. *Chem Eng J.* **2021**;420: 127720.
 39. Zhu SM, Kang ZX, Wang F, Long Y. Copper nanoparticle decorated non-woven polypropylene fabrics with durable superhydrophobicity and conductivity. *Nanotechnology.* **2021**;32: 035701.
 40. Hasan MM, Zhu FC, Ahmed A, Khoso NA, Deb H, Lai YC, Islam MZ, Sun H, Yu B. Functionalization of polypropylene nonwoven fabrics using cold plasma (O₂) for developing graphene-based wearable sensors. *Sensor Actuat A-Phys.* **2019**;300: 111637.
 41. Jiao KY, Zhu T, Li XH, Shan MJ, Xu ZW, Jiao YN. Assembly of graphene oxide on nonconductive nonwovens by the synergistic effect of interception and electrophoresis. *J Nanopart Res.* **2015**;17:373.
 42. Li YJ, Nie M, Wang Q. Facile fabrication of electrically conductive low-density polyethylene/carbon fiber tubes for novel smart materials via multiaxial orientation. *ACS Appl Mater Interfaces.* **2018**;10:1005.
 43. Weng BC, Xu FH, Salina A, Lozano K. Mass production of carbon nanotube reinforced poly(methyl methacrylate) nonwoven nanofiber mats. *Carbon.* **2014**;75:217.
 44. Liu H, Li QM, Bu YB, Zhang N, Wang CF, Pan CF, Mi LW, Guo ZH, Liu CT, Shen CY. Stretchable conductive nonwoven fabrics with self-cleaning capability for tunable wearable strain sensor. *Nano Energy.* **2019**;66: 104143.
 45. Jiang XP, Ren ZL, Fu YF, Liu YF, Zou R, Ji GP, Ning HM, Li YQ, Wen J, Qi HJ, Xu CH, Fu SY, Qiu JH, Hu N. Highly compressible and sensitive pressure sensor under large strain based on 3D porous reduced graphene oxide fiber fabrics in wide compression strains. *ACS Appl Mater Interfaces.* **2019**;11:37051.
 46. Tao LQ, Zhang KN, Tian H, Liu Y, Wang DY, Chen YQ, Yang Y, Ren TL. Graphene-paper pressure sensor for detecting human motions. *ACS Nano.* **2017**;11:8790.
 47. Kim KH, Hong SK, Jang NS, Ha SH, Lee HW, Kim JM. Wearable resistive pressure sensor based on highly flexible carbon composite conductors with irregular surface morphology. *ACS Appl Mater Interfaces.* **2017**;9:17499.
 48. Guo Y, Guo ZY, Zhong MJ, Wan PB, Zhang WX, Zhang LQ. A flexible wearable pressure sensor with bioinspired microcrack and interlocking for full-range human-machine interfacing. *Small.* **2018**;14:1803018.
 49. Lee JH, Kim E, Zhang H, Chen HM, Venkatesan H, Chan KY, Yang J, Shen X, Yang JL, Jeon S, Kim JK. Rational design of all resistive multifunctional sensors with stimulus discriminability. *Adv Funct Mater.* **2021**;32:2107570.
 50. Chun SW, Son W, Choi C. Flexible pressure sensors using highly-oriented and free-standing carbon nanotube sheets. *Carbon.* **2018**;139:586.
 51. Song Y, Chen HT, Su ZM, Chen XX, Miao LM, Zhang JX, Cheng XL, Zhang HX. Highly compressible integrated supercapacitor-piezoresistance-sensor system with CNT-PDMS sponge for health monitoring. *Small.* **2017**;13:1702091.
 52. Yao HB, Ge J, Wang CF, Wang X, Hu W, Zheng ZJ, Ni Y, Yu SH. A flexible and highly pressure-sensitive graphene-polyurethane sponge based on fractured microstructure design. *Adv Mater.* **2013**;25:6692.
 53. Zhao X, Wang WL, Wang Z, Wang JG, Huang T, Dong J, Zhang QH. Flexible PEDOT: PSS/polyimide aerogels with linearly responsive and stable properties for piezoresistive sensor applications. *Chem Eng J.* **2020**;395: 125115.
 54. Liu H, Chen XY, Zheng YJ, Zhang DB, Zhao Y, Wang CF, Pan CF, Liu CT, Shen CY. Lightweight, superelastic, and hydrophobic polyimide nanofiber/MXene composite aerogel for wearable piezoresistive sensor and oil/water separation applications. *Adv Funct Mater.* **2021**;31:2008006.
 55. Wu XD, Han YY, Zhang XX, Zhou ZH, Lu CH. Large-area compliant, low-cost, and versatile pressure-sensing platform based on microcrack-designed carbon black@polyurethane sponge for human-machine interfacing. *Adv Funct Mater.* **2016**;26:6246.
 56. Lu LJ, Jiang CP, Hu GS, Liu JQ, Yang B. Flexible noncontact sensing for human-machine interaction. *Adv Mater.* **2021**;33:2100218.

Publisher's Note Springer Nature remains neutral with regard to jurisdictional claims in published maps and institutional affiliations.

Springer Nature or its licensor (e.g. a society or other partner) holds exclusive rights to this article under a publishing agreement with the author(s) or other rightsholder(s); author self-archiving of the accepted manuscript version of this article is solely governed by the terms of such publishing agreement and applicable law.



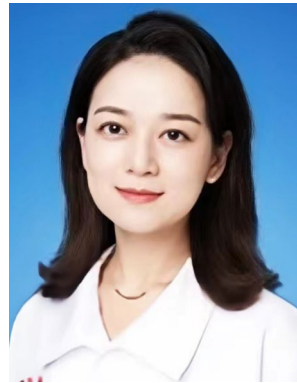
Guangliang Tian received his B.S. degree (in 2016) from Dalian Polytechnic University, China. He is currently pursuing the Ph.D. degree at Donghua University under the guidance of Prof. Qinfei Ke and Prof. Chen Huang. His research interests mainly focus on multifunctional fibers and nonwovens for flexible electronics textiles.



Leihang Yang received his B.S. degree (in 2021) from Taiyuan University of Technology, China. He is currently a master student at College of Textile, Donghua University. His research interests mainly focus on solar-driven fiber-based interfacial evaporators.



Yihan Shi received her B.S. degree (in 2020) and M.S. degree (in 2023) from Donghua University, China. Her research interests mainly focus on the structural design and fabrication of functional nonwovens for environmental protection.



Yi Lu Ph.D., is a physician in Shanghai Jiao Tong University affiliated sixth people's hospital, China. Her clinical interests are pulmonary diseases, with a focus on pulmonary fibrosis and blood gas analysis. She has been a principle investigator in numerous clinical trials, with a focus on wearable devices of the real-time monitoring of physiological information.



Jixia Deng received her B.S. degree (in 2019) from Donghua University, China. She is currently a Ph.D. candidate in Textile Engineering, Donghua University. Her major research interests focus on nonwovens and biomedical materials.



Yi Zhao received her M.S. degree (in 2011) from Donghua University, China, Ph.D. degree (in 2015) and Postdoctoral Research Fellow (in 2016) from University of Nebraska-Lincoln, America. Currently, she is an associate professor of nonwoven materials and engineering in College of Textiles, Donghua University. Her research interests include controlled-release fragrance nonwoven materials, functional air filtration nonwoven materials and nonwoven renewable raw materials.



Wenhua Yu received her B.S. degree (in 2020) from Donghua University, China. She is currently a Ph.D. candidate in Textile Engineering, Donghua University. Her major research interests focus on nonwovens and flexible sensors.



Xiangyu Jin is currently a full professor at the College of Textiles, Donghua University, China. He is a vice director of the Engineering Research Center of Technical Textiles, Ministry of Education, China. His research interests include geosynthetic materials, multifunctional air filtration nonwovens, degradable and dispersible nonwovens, new nonwoven technology, nonwoven manufacturing and industrialization.

construction, international exchange and cooperation, and has published many management papers.



Chen Huang received his B.S. degree (in 2007) and Ph.D. degree (in 2013) from Donghua University, China. Currently, he is a professor at the College of Textiles, Donghua University. His research interests include functional nonwovens, fibrous materials and biomedical textiles. He has published more than 100 papers and has been granted more than 20 Chinese patents.



Qinfei Ke received her Ph.D. degree (in 2000) from Donghua University, China. Currently, she is a professor at the College of Textiles, Donghua University. She is mainly engaged in research on eco-environmental materials, biomedical materials and higher education management. She has presided over and participated in nearly 30 national 863 projects, National Natural Science Foundation projects, provincial and ministerial projects and enterprise projects. She has rich practice and experience

in higher education management, such as teaching management, faculty